Use of methyl esterified eggshell membrane for treatment of aqueous solutions contaminated with anionic sulfur dye

Hee-Jeong Choi

ABSTRACT

The present study assessed the adsorption of an anionic dye (sulfur blue) by methyl-esterified eggshell membrane (MESM), a low-cost and abundant material from waste. Adsorption kinetics were investigated using parameters such as pH, contact time, initial dye concentration, solution temperature, dosage of adsorbent, and particle size of adsorbent. After methyl esterification, the specific surface area significantly increased and the negative surface charge of the eggshell membrane changed to positive for all pH values, which increased the sulfur dye sorption capacity. The optimal conditions for sorption of sulfur dye onto MESM resulted in >98% removal and were as follows: <35 μm particle size, pH 8, 20 min contact time and 313 K temperature. In this respect, 0.68–0.73 dry weight mg/L sulfur dye was adsorbed per 1 mg/L MESM. The Langmuir adsorption capacity for sulfur dye was 187.6 mg/g. In addition, sulfur removal was spontaneous and uptake was endothermic. MESM is an inexpensive and effective adsorbent.

Key words | adsorption, anionic dye, eggshell membrane, kinetics, methyl esterification

Hee-Jeong Choi
Department of Energy and Environment Convergence,
Catholic Kwandong University,
Beomil-ro 579,
Gangneung,
Korea
E-mail: *hjchoi@cku.ac.kr*

INTRODUCTION

The textile dying industry consumes around 100–1,100 million tons of various dyestuffs every year in the world and produces large volumes of wastewater including different hazardous chemicals (Choi & Kim 2016). The dyeing wastewater comprises around 2–5% of various dyestuffs and this corresponds to about 2–5 million tons (Işmal *et al.* 2014). In particular, reactive dyes and sulfur dyes release ca. 20–50% dyestuffs into wastewater through the dyeing process, whereas basic dyes, disperse dyes and acid dyes release ca. 0–5% dyestuffs into wastewater (Nguyen & Juang 2013). Half of the volume of all dyes used on cellulosic fibers is sulfur dyes, of which approximately 80% are black sulfur dyes (Ghaly *et al.* 2014).

The treatment of dyeing wastewater is not easy because dyes are mainly aromatic and heterocyclic compounds. The structure of dyes is complex, stable and not biodegradable in the solution (Ghaly *et al.* 2014). Thus, the most effective methods and technologies for dye removal involve the adsorption method based on activated carbon. However, this process is costly and the adsorbents are difficult to regenerate after use (Choi & Kim 2016). Therefore, development of a cost-effective, eco-friendly technology for treatment of textile dyeing wastewater is necessary.

The Korean food industry produces 90,000 tons of eggshell waste per year. Of this 26.2% is used as fertilizer, 10.7% as animal feed ingredients, 3.2% for other uses, and the remainder is discarded as waste (Choi & Lee 2015). However, many landfill operators are reluctant to accept eggshell waste because the eggshells and the attached membrane attract pests. Eggshell membrane (ESM) has good adsorbent properties, including the ability to remove heavy metals and dyes from wastewater (Guru & Dash 2014). In general ESM is positively charged at pH 1–6 and negatively charged at pH 6–12 (Chen *et al.* 2012). The surface property of the ESM dominates its sorption behaviors toward various ions and species. However, the negatively charged carboxylic groups inhibit the adsorption of anion ions by ESM (Tsai *et al.* 2006). To overcome these problems the ESM surface charge property is changed according to the esterification of carboxylic groups, which is the main driver of improved dye sorption capacity. Methyl-esterified eggshell membrane (MESM) has a high

doi: 10.2166/wst.2017.346

cationic charge density and can thus strongly adsorb and destabilize negative particles, such as negatively charged sulfur dyes. MESM from eggshell waste has been recommended for use as an adsorbent because of its low cost, copious availability, non-toxicity, high specific surface area, biodegradability, high potential for ion exchange for charged pollutants, and safe handling (Chen *et al.* 2013). Moreover, MESM can be regenerated and reused several times. Biological, chemical, and physical processes for heavy metal removal using eggshell (Rohaizar *et al.* 2013; Pettinato *et al.* 2015) and ESM (Chen *et al.* 2012, 2013) have been reported. However, no examination of MESM for removal of sulfur dyes has been reported. Therefore, the novelty of this study is its proposal of effective use of MESM for removal of sulfur dye from aqueous solution. We expect MESM to be used as an eco-friendly adsorbent in place of other chemical dye-removal agents.

MATERIALS AND METHODS

Materials

Waste eggshell samples were collected from a chicken farm in Gangneung City, Korea. To remove all adhering and interfering materials, such as organics and salts, the samples were rinsed several times with deionized water and then boiled in water. After cleaning, the eggshells were dried in an oven at 80 °C for 24 h. The dried eggshells were first pretreated with 15% (v/v) HCl overnight to dissolve the outer layer of the shell and leave the ESM. The separated ESM was then cleaned using deionized water, dried at 80 °C for 24 h in an oven, and crushed into fine powder using a mortar and pestle for future use. Thereafter, 100 mg of the pretreated ESM powder was immersed in 50 mL methanol containing 2% (v/v) HCl for 10 h at 80 °C to esterify carboxylic groups in the ESM structure. The resultant MESM was rinsed several times with deionized water, dried at 80 °C for 24 h in an oven, and stored in a desiccator for future use.

Sulfur blue 11 (CI 53235 and molecular weight 305 g/mol; Tera Pharmaceuticals Inc., Buena Park, USA) was used as anionic dye for adsorption onto ESM and MESM. The sulfur dyes were adsorbed by cotton from a bath containing sulfide and insolubilized within the fiber by oxidation (Ding *et al.* 2010). Therefore in this study, the water-soluble form of sulfur blue was generated by alkaline reduction with sodium sulfide.

Experimental design

The sulfur dye removal onto MESM was investigated using various parameters, such as particle size, pH and temperature. In addition adsorption kinetics using a pseudo-second-order model, adsorption isotherm using Langmuir and Freundlich, and adsorption thermodynamics were analyzed. The experiment was carried out in the form of a batch-test. For the effect of MESM on sulfur dye removal, an MESM particle size of 20–100 μm, initial sulfur dye concentration of 1–40 mg/L, and MESM doses of 1–30 mg/L were added in various concentrations of sulfur dye contained in 1 L water. The suspension was shaken for various lengths of time (1–120 min) with controlled pH. The pH was controlled from 1 to 12 using NaOH and/or H_2SO_4, and a temperature range of 283–313 K was used to assess the effect of temperature. Defined amounts of MESM were added to aqueous solutions of sulfur blue, and the suspension was shaken for varying lengths of time. At the end of the run, the suspension was centrifuged at 1,500 rpm (628 *g*) for 20 min. Supernatant was removed at predetermined time points from the middle of the dye suspension and filtered through a 0.45 μm membrane filter (Watman, Sigma-Aldrich) to separate the filtrate and adsorbent residue. All experiments were carried out by changing one parameter at a time while holding the others constant.

Analytical methods

The Brunauer–Emmett–Teller (BET) surface area of the samples was determined using a Protech Korea BET surface area analyzer (Model ASAP 2020). The particle size and amount of sericite were analyzed using laser diffraction (Laser Diffraction Master Class 3&4, Malvern, UK) and micro scales (XP26, Mettler Toledo, Switzerland), respectively. Zeta potential measurements of ESM and MESM in aqueous solution were conducted using a Malvern Zetasizer Nano-Z analyzer (Malvern, UK). A scanning electron microscope (SM-300, Topcon, Japan) with an energy dispersive spectroscope (EDS spectrometer, Shimadzu, Japan) was used for surface imaging and elemental analysis of MESM and ESM. The point of zero charge (PZC) of the adsorbent was determined by the solid addition method. A detailed measurement method of PZC is given in the literature (Bertolini *et al.* 2013). The absorbance of filtered samples was measured at the peak wavelength of dye (λ_{max} sulfur blue = 620 nm) using a UV-2550 UV-visible spectrophotometer (Shimadzu, Japan). The adsorption capacity was

calculated using the equation below:

$$q_e = \frac{\{(C_0 - C_e)V\}}{m} \quad (1)$$

where q_e (mg/g) is the adsorption capacity, the dye uptake by a unit weight of adsorbent; C_0 (mg/L) is the initial concentration of dye; C_e (mg/L) is the residual concentration; V (L) is the volume of solution and m (g) is the weight of adsorbent.

Removal efficiency (%) was calculated to investigate the percentage of dye removal as follows:

$$R = \left\{\frac{(C_0 - C_e)}{C_0}\right\} \times 100\% \quad (2)$$

where R (%) is the removal ratio, C_0 (mg/L) is the initial concentration of dye and C_e (mg/L) is the residual concentration of dye. The high cationic charge density of MESM allows it to strongly adsorb the negatively charged regions of sulfur dyes. All experiments were repeated five times, and average results are presented.

RESULTS AND DISCUSSION

Characterization of ESM and MESM

Scanning electron microscopic (SEM) images of ESM samples before and after methyl esterification are shown in Figure 1(a) and 1(b), respectively. The SEM images of ESM and MESM demonstrate similar morphologies. MESM has a porous structure similar to ESM; however, it is composed of a network of fibrous proteins, such as collagen type, (Figure 1), and the specific surface area was increased which would enable adsorption of the sulfur dye in aqueous solution. ESM contains various organic/inorganic matter and minerals. Chen *et al.* (2013) reported that the C, N, and S contents in ESM were 42.6, 31.5, and 9.9%, respectively. In this study after methyl esterification, the contents of C, N and S were determined as 54.7, 20.4, and 7.4%, respectively. The increase in C and decreases in N and S further indicated the esterification of carboxylic groups on the ESM surface.

The BET specific surface area, pore volume and pore size for ESM and MESM are shown in Table 1. The pore size and pore volume of ESM were significantly increased after methyl esterification. Moreover, the activation caused a marked increase in specific surface area from 4.45 to 57.62 m^2/g.

The PZC is defined as the pH at which the surface of the adsorbent has neutral charge. The pH_{pzc} adsorbents depend on several factors such as the nature of crystallinity, impurity content, temperature, adsorption efficiency of electrolytes, and degree of adsorption of H^+ and OH^- (Appel *et al.* 2003). At $pH = pH_{pzc}$ sulfur dye was adsorbed on ESM even though the surface charge was neutral, indicating the sulfur dye was adsorbed by other mechanisms than electrostatic attraction. The value of pH_{pzc} of ESM was lower than the pH in water indicating that the surface presented a negative charge in aqueous solution ($pH > pH_{pzc}$). The value of the pH_{pzc} of ESM obtained in this study was 6.3 (Table 2). The value is lower than the pH and the surface of ESM also showed negative charge.

ESM and MESM surfaces are shown in Figure 2. The ESM surface was positively charged at pH 1–6 and negatively charged at pH > 6. However, MESM was positively charged over the entire pH range. The potential of MESM was

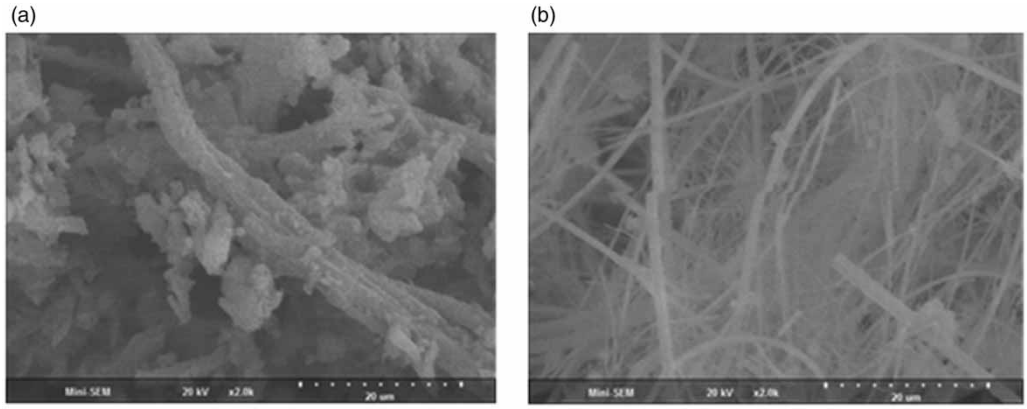

Figure 1 | SEM images of ESM (a) and MESM (b).

Table 1 | Textural properties of ESM and MESM

Materials	BET specific surface area (m^2/g)	Pore size (nm)	Pore volume (cm^3/g)
ESM	4.45	3.45	0.069
MESM	57.62	6.43	0.110

Table 2 | Physico chemical characteristics of ESM

Parameters	pH	Electrical conductance (mS)	Specific gravity	Moisture content (%)	pH_{zpc}
ESM	6.59	0.1	0.846	1.174	6.31

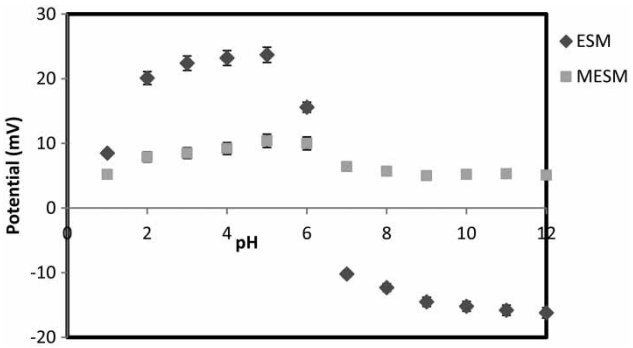

Figure 2 | Surface potential of ESM and MESM according to pH (dosage of ESM: 10 mg/L and MESM: 10 mg/L).

5–10 mV at all pH values, whereas that of ESM varied from 23.7 to −16.2 mV over all pH values and changed significantly at pH 6. The negatively charged carboxylic groups present on ESM inhibit the adsorption of anion species (Nguyen & Juang 2013). After methyl esterification, the negative surface charge property of ESM is changed to positive at all pH values, which improves the sulfur dye sorption capacity. In general, potential values of ±5 mV represent rapid adsorption, while values from ±10 to ±30 mV represent unstable adsorption (Choi 2015). In this study, the MESM potential for all pH ranges was in the range of 0–8 mV.

Effect of pH

The pH factor is an important parameter in the dye adsorption process. The pH of an aqueous solution will control the magnitude of electrostatic charges which are imparted by the ionized dye molecules (Choi & Kim 2016). Sulfur dye removal efficiency was determined according to pH (Figure 3). The removal efficiency of sulfur dye by ESM

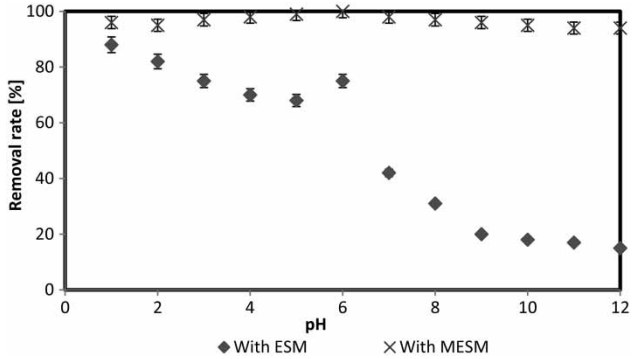

Figure 3 | Removal of sulfur blue by natural ESM and MESM according to pH (C_0: 5 mg/L, particle diameter: <35 μm, mixing speed (S): 500 rpm (50 min), T: 313 K and MESM dose (m_s): 10 mg/L).

was strongly dependent on pH. The removal rate of sulfur dye by ESM decreased with increasing pH: removal rate of 88 to 70% below pH 6 and 42 to 15% at pH 7–12. In contrast, the removal efficiency of sulfur due by MESM remained constant at 94–100% at all pH values. This result was related to the pH_{pzc} value of ESM and MESM. The negatively charged surface of ESM exhibited low adsorption of negatively charged sulfur dye up to pH 7. However, positively charged MESM adsorbed a significant quantity of negatively charged sulfur blue. The optimum pH for sulfur dye adsorption by MESM was 5–7. This difference was likely due to the lower anion exchange capacity of ESM. It is interesting to note that anion exchange is restricted to the surface and edges of the ESM particles. In general, the model was able to predict adsorption decay during the very early stages of adsorption. Dye uptake was highly sensitive to pH changes in the adsorption system (Abidi *et al.* 2015). The adsorption capacity of ESM has been reported previously (Daraei *et al.* 2013; Rohaizar *et al.* 2013). The adsorption of metal ions by ESM is strongly dependent upon the conditions. In particular, pH affects binding site protonation, calcium carbonate solubility and metal speciation. To overcome these problems, ESM was esterified with methylene. The adsorption of sulfur dye by MESM was highly effective in the wide range of pH.

Effect of parameters

Effect of particle size range according to contact time

The particle size of adsorbent is an important parameter for removal of sulfur dye in the aqueous solution using MESM because it significantly depends on the available binding sites of the MESM surface. The adsorption of sulfur blue

onto MESM is shown in Figure 4(a). Equilibrium was reached in a very short time for all samples. The adsorption capacity decreased with increasing particle size. A particle size range of <35 μm resulted in adsorption of 99.38% of sulfur blue onto MESM, compared to 87.5, 75.63 and 69.38% for 36–60, 61–75 and 76–100 μm particle size ranges, respectively. This indicated that surface area increases with decreasing MESM particle size for a given mass of MESM; as a consequence the number of binding sites increases. The initial sorption rate also decreased with increasing particle size. This is expected because the external surface area available for reaction decreased with increasing particle size for a constant adsorbent mass. The contact time could influence process performance. An increase in contact time generally enhances sulfur dye removal; however, the ion retro-dissolution phenomenon could take place (Pettinato *et al.* 2015). As a result, adsorption equilibrium was reached more rapidly with decreasing MESM particle size. However, all MESM particle size ranges achieved adsorption equilibrium in ca. 20 min.

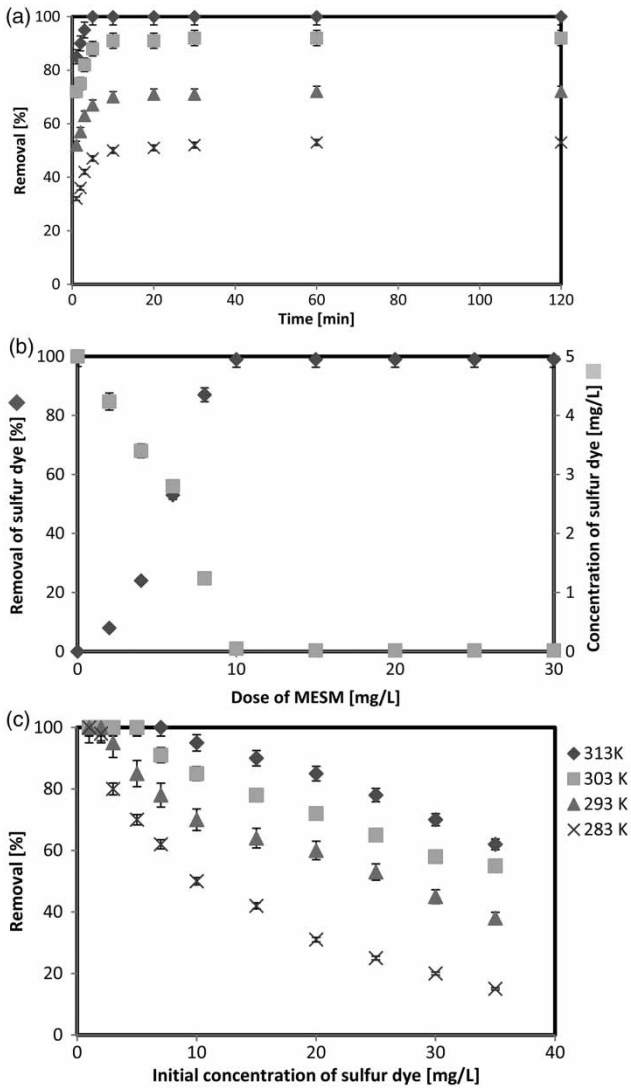

Figure 4 | (a) Effect of MESM particle size on sulfur dye removal (particle size: <35 μm (◆), 36–60 μm (■), 61–75 μm (▲), 76–100 μm (X), C_0: 5 mg/L, pH: 8, S: 500 rpm, T: 313 K and m_s: 10 mg/L). (b) Effect of MESM dose on sulfur dye removal (particle size: <35 μm, C_0: 5 mg/L, pH: 8, S: 500 rpm, T: 313 K and m_s: 10 mg/L). (c) Effect of initial concentration and temperature on sulfur dye removal (particle size: >35 μm, pH: 8, S: 500 rpm and m_s: 10 mg/L).

Effect of MESM dose

Adsorbent dosage is also an important influencing parameter for the adsorption process. In general, as the quantity of ESM increases, the specific surface area and dye binding sites also increase. However, excessive amounts of the adsorbents may result in particle aggregation, overlapping and overcrowding, resulting in a decrease in surface area and sorption capacity (Pettinato *et al.* 2015). Therefore, optimization of adsorbent dosage is necessary to reduce the cost and to increase the adsorption capacity. The results indicated that the sulfur dye removal rate increased with increasing MESM dose and sulfur dye removal of 99% was achieved using 10 mg/L MESM (Figure 4(b)). Therefore, approximately 0.68–0.73 dry weight mg/L sulfur dye was adsorbed per 1 mg/L MESM. The most efficient method of dye removal is based on adsorption from solution onto activated carbon. However, this is expensive and the adsorbent is difficult to regenerate after use (Choi 2015). Another efficient method of dye removal is flocculation. Despite its high efficiency, flocculation requires a large quantity of chemicals and high cost. For example, the typical dose of ferric salt required for flocculation was >500 mg/L (Kim *et al.* 2015); and the cost of chitosan is $10–1,000 per kilogram, depending on the product quality (Mahe *et al.* 2015). However, MESM is an alternative inorganic adsorbent that has several advantages, including low cost, abundant availability, non-toxicity and high pollutant adsorption capacity. The anion and organic matter adsorption capacity is high because of MESM's colloidal properties and positively charged layers. Therefore, MESM may represent an alternative environmentally friendly absorbent.

Effect of temperature

The temperature dependence of the sorption rate was reflected by the extremely high correlation coefficient (Table 3). The effect of initial sorptive concentration was determined by varying the initial concentration of sulfur

Table 3 | Langmuir and Freundlich parameters for sulfur dye removal

Temperature (K)	Langmuir			Freundlich		
	q_0 (mg/g)	K_L (L/g)	R^2	$1/n$	K_F (mg/g)	R^2
283	67.5	2.852	0.998	0.164	3.615	0.987
293	87.4	3.021	0.996	0.171	4.327	0.983
303	148.5	3.742	0.998	0.187	4.859	0.984
313	187.6	4.370	0.999	0.203	5.569	0.975

dye from 1 to 35 mg/L at pH 8. The sorption data for sulfur dye at 283, 293, 303 and 313 K are shown in Figure 4(c). The sulfur dye sorption capacity increased with decreasing initial concentration. The percent removal decreased gradually because fewer active sites were available as the initial concentration of sulfur dye increased. Indeed, the amount adsorbed by MESM increased with increasing initial concentration of sulfur dye (Figure 4(c)). Moreover, the amount of sulfur dye removed increased significantly with increasing temperature. The sorption capacity decreased from 188 to 68 mg/g as the temperature decreased from 313 to 283 K. The increase in the equilibrium sorption of sulfur dye with temperature indicates that a high temperature favors sulfur dye removal by sorption to MESM due to enhanced escape of sulfur dye from the interface.

Adsorption isotherm

The concentration dependence data at equilibrium between MESM and the solution interface were further analyzed using the Langmuir (Equation (3)) and Freundlich (Equation (4)) adsorption isotherm models (Lalhmunsiama & Lee 2016):

$$\frac{C_e}{q_e} = \frac{1}{(q_0 K_L)} + \frac{C_e}{q_0} \tag{3}$$

$$\log q_e = \frac{1}{n}\log C_e + \log K_F \tag{4}$$

where q_e is the amount of solute adsorbed per unit weight of adsorbent (mg/g), C_e is the equilibrium bulk concentration (mg/L), q_0 is the Langmuir monolayer adsorption capacity (mg/g) and K_L is the Langmuir constant (L/g). K_F and $1/n$ are the Freundlich constants, referring to adsorption capacity and adsorption intensity, respectively. Straight lines with fairly good fits were obtained for the two isotherms; the isotherm constants and the associated R^2 values are shown in Table 3.

The regression coefficients (R^2) of Langmuir were a better fit than those of the Freundlich adsorption model for sulfur dye removal. The K_L value increased with increasing temperature. This may be due to the fact that the reaction activity between sulfur dye and MESM was increased with increasing temperature. Therefore, a high temperature is more effective for sulfur dye removal by MESM. Higher values of Langmuir constant and Freundlich sorption capacity obtained may further confirm the strength and affinity of the employed MESM towards the sulfur dye (Lalhmunsiama & Lee 2016). The fractional value of $1/n$ with the Freundlich isotherm for sulfur dye was $0 < 1/n < 1$, suggesting that the MESM has a heterogeneous surface structure of active sites. The $1/n$ value increased within the range of 0–1 with increasing temperature. This means that the Freundlich isotherm becomes more linear with increasing temperature. The Freundlich isotherm is linear if $1/n = 1$ and, becomes more nonlinear if $1/n$ decreases (Coles & Yong 2006). Relatively straight lines were obtained between C_e/q_e versus C_e for the Langmuir model (Figure 5(a)) and log q_e versus log C_e for the Freundlich model (Figure 5(b)). This suggests that the interactions of sulfur dye with the MESM surface are chemical in nature.

The Langmuir sorption capacities of various low-cost materials for anionic dye are shown in Table 4. The sorption capacities varied due to differences in the physicochemical properties of adsorbents. MESM has a lower adsorption capacity than microgel or SBA-16. However, MESM has a higher adsorption capacity compared with kaolinite, montmorillonite, and bentonite. In particular, the adsorption capacity of MESM was 1.67- to 4.59-fold higher than that of ESM. MESM has the advantages of use of waste materials, waste recycling and reduction in landfill cost.

Adsorption kinetics

A fast absorption rate and large absorption capacity are important criteria for a better choice of material to be used as a good absorbent. The dynamics of the adsorption can be studied by the kinetics of adsorption in terms of the order of the rate constant (Lalhmunsiama & Lee 2016). In this study pseudo-second-order (Equation (5)) kinetic models were exploited to obtain the sorption kinetics of sulfur dye on MESM. The equations were used in linear form:

$$\frac{t}{q_t} = \frac{1}{(kq_e^2)} + \frac{t}{q_e} \tag{5}$$

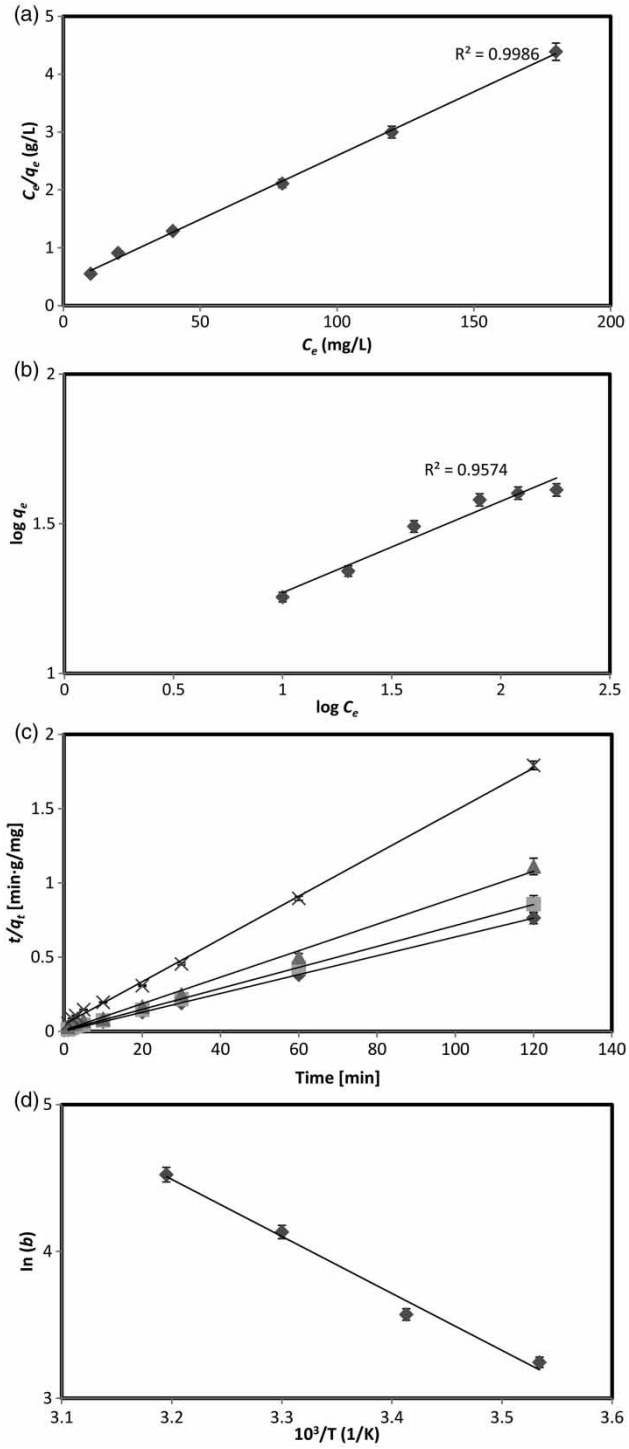

Figure 5 | (a) Langmuir adsorption isotherm for sulfur dye according to sorptive concentration (particle size: >35 μm, pH: 8, S: 500 rpm, T: 313 K); (b) Plot of log q_e versus log C_e for sulfur dye on MESM (particle size: <35 μm, pH: 8, S: 500 rpm, T: 313 K); (c) Pseudo-second-order sulfur dye adsorption kinetics of MESM particles of various sizes: <35 μm (◆), 36–60 μm (■), 61–75 μm (▲) and 76–100 μm (X) (C_0: 5 mg/L, pH: 8, S: 500 rpm (50 min), T: 313 K and m_s: 10 mg/L; (d) Plot of ln(*b*) against temperature for sulfur dye sorption on MESM.

Table 4 | Anionic dye removal by low-cost materials

Adsorbate	Adsorbent	q_m (mg/g)	Reference
Basic Red 2	SBA-16	240.39	Chaudhuri *et al.* (2016)
Basic Red 5	SBA-16	276.24	Chaudhuri *et al.* (2016)
Congo red 4BS	Microgel	869.1	Jin *et al.* (2015)
Acid red GR	Microgel	1,469.7	Jin *et al.* (2015)
Reactive light yellow	Microgel	1,250.9	Jin *et al.* (2015)
Sulfur blue	Kaolinite	2.3	Nguyen & Juang (2013)
Sulfur blue	Montmorillonite	2.6	Nguyen & Juang (2013)
RR120	Fouchana	9.7	Errais *et al.* (2011)
RR120	Bentonite	2.8	Errais *et al.* (2011)
Malachite green	ESM	89.72	Chen *et al.* (2012)
Organic dye eosin B	ESM	40.9	Ning & Tao (2011)
Congo Red	ESM	112.3	Liu *et al.* (2012)
Sulfur blue	MESM	187.6	Present study

q_m: maximum adsorption capacity.

where q_e (mg/g) is the maximum sorption capacity, q_t (mg/g) is the amount adsorbed at time t, and k (g/(mg min)) is the adsorption rate constant of the pseudo-second-order equation. Linear plots of the t/q_t by t in Figure 5(c) showed the applicability of the pseudo-second-order equation for the sulfur dye with MESM particle of size ranges from <38 to 76–100 μm. The correlation coefficients for the linear plots of t/q_t against time from the pseudo-second-order rate law are greater than 0.994 for all systems for a contact time of 120 min. This result, with the pseudo-second-order model based on the adsorption capacity on the solid phase, suggests that the adsorption of the sulfur dyes onto MESM is controlled by chemisorption involving valence forces through sharing or exchange of electrons between adsorbent and adsorbate (Arshadi *et al.* 2014).

The calculated parameters for the effect of particle size on and sulfur blue absorption are shown in Table 5. The pseudo-second-order constant (k) decreased with increasing particle size and initial concentration and increased with increasing temperature. These data suggest that sulfur blue removal by MESM increased with decreasing particle size and concentration and increasing temperature. The reaction of small MESM particles was more rapid than that of larger particles because the external surface area available

Table 5 | Effect of particle size, temperature and initial concentration on dye removal

Particle size (μm)	R^2	q_e (mg/g)	k ($\times 10^{-3}$ g/mg·min)
>35	1.000	157	22.3
36–60	0.998	138	17.17
61–75	0.999	110	8.22
76–100	0.994	95	2.57
Temperature (K)			
283	1.000	56.2	1.14
293	0.999	60.13	1.24
303	0.998	67.45	1.31
313	1.000	84.5	1.53
Initial concentration (mg/L)			
50	1.000	33.33	20.52
100	1.000	67.57	12.31
150	0.997	93.75	7.62
200	0.999	125.05	3.82
250	0.998	138.89	2.02
300	0.998	157.89	1.59

decreased with increasing particle size for a constant sorbent mass. The sorption capacity of MESM increased from 33.33 to 157.89 mg/g as the initial dye concentration increased from 50 to 300 mg/L. The pseudo-second-order equation and regression coefficients for the linear plots were higher than 0.994 for MESM and is shown in Table 5.

Adsorption thermodynamics

The van 't Hoff analysis was used to assess the spontaneity of the adsorption of dyes on MESM:

$$\ln b = \frac{\Delta S}{R} - \frac{\Delta H}{RT} \tag{6}$$

$$\Delta G = \Delta H - T\Delta S \tag{7}$$

where ΔH is the change in enthalpy (J/mol), ΔS is the change in entropy (J/(mol K)), ΔG is the change in Gibbs free energy (J/mol), b is the Langmuir gas constant at temperature T (K) and R is the universal gas constant (8.314 J/(mol K)). The ΔS and ΔH values were evaluated from the intercept and slope of the plot of ln b vs. 1/T (Figure 5(d)). The positive ΔH (29.31 kJ/mol) values suggest that the process is endothermic (Chen *et al.* 2013) and the positive ΔS (0.1123 kJ/(mol K)) values reveal an increase in randomness at the solid–solution interface during dye adsorption on the active sites of MESM adsorbent. The ΔG was −2.443, −3.572, −4.705 and −5.826 kJ/mol as the temperature increased to 283, 293, 303 and 313 K, respectively. The decrease of Gibbs free energy with increasing temperature indicates a better adsorption at higher temperature (Singha & Das 2011). Moreover the negative ΔG values confirm the spontaneous nature of the dye uptake process.

CONCLUSIONS

The carboxyl groups on ESM were esterified with methanol containing 2% (v/v) HCl for 10 h at 80 °C to produce green adsorbent MESM. After esterification the specific surface area significantly increased from 4.45 to 57.62 m^2/g and the negative surface charge was changed to positive at all pH values, which improved the sulfur dye sorption capacity. The optimal conditions for sorption of sulfur dye onto MESM (maximum 98% removal) were as follows: <35 μm particle size, pH 8, 20 min contact time and 313 K. Under these conditions, approximately 0.68–0.73 dry weight mg/L sulfur dye was adsorbed per 1 mg/L MESM. Equilibrium sorption data for sulfur dye fitted well to the Langmuir adsorption isotherms and the kinetic data fitted reasonably well to the pseudo-second-order kinetic model. Further, an increase in temperature favored sulfur dye removal, and the sorption process was found to be spontaneous and endothermic in nature. After methyl esterification of ESM, the surface chemistry is more favorable for adsorption of sulfur dyes. Its environmentally friendliness, low dose requirement and high removal efficiency are the advantages of MESM over commonly used adsorbents.

ACKNOWLEDGEMENTS

This study was supported by the Basic Science Research Program through the National Research Foundation of Korea (NRF) funded by the Ministry of Education, Science and Technology (2016005271).

REFERENCES

Abidi, N., Errais, E., Duplay, J., Berez, A., Jrad, A., Schäfer, G., Ghazi, M., Semhi, K. & Trabelsi-Ayadi, M. 2015 Treatment of dye-containing effluent by natural clay. *J. Clean. Prod.* **86**, 432–440.

Appel, C., Ma, L. Q., Rhue, R. D. & Kennelley, E. 2003 Point of zero charge determination in soils and minerals via traditional methods and detection of electroacoustic mobility. *Geoderma* **113**, 77–93.

Arshadi, M., Amiri, M. J. & Mousavi, S. 2014 Kinetic, equilibrium and thermodynamic investigations of Ni(II), Cd(II), Cu(II) and Co(II) adsorption on barley straw ash. *Water Resour. Ind.* **6**, 1–17.

Bertolini, T. C. R., Izzidoro, J. C., Magdalena, C. P. & Fungaro, D. A. 2013 Adsorption of crystal violet dye from aqueous solution onto zeolites from coal fly and bottom ashes. *Orbital Electron. J. Chem.* **5** (3), 179–191.

Chaudhuri, H., Dash, S., Ghorai, S., Pal, S. & Sarkar, A. 2016 SBA-16: Application for the removal of neutral, cationic, and anionic dyes from aqueous medium. *J. Environ. Chem. Eng.* **4**, 157–166.

Chen, H., Liu, J., Cheng, X. & Peng, Y. 2012 Adsorption for the removal of malachite green by using eggshell membrane in environment water sample. *Adv. Mater. Res.* **573–754** 63–67.

Chen, M. L., Gu, C. B., Yang, T., Sun, Y. & Wang, J. H. 2013 A green sorbent of esterified egg-shell membrane of highly selective uptake of arsenate and speciation of inorganic arsenic. *Talanta* **116**, 688–694.

Choi, H. J. 2015 Effect of Mg-sericite flocculant for treatment of brewery wastewater. *Appl. Clay Sci.* **115**, 145–149.

Choi, H. J. & Kim, K. H. 2016 Parametric study of a dyeing wastewater treatment by modified sericite. *Environ. Technol.* **37** (20), 2572–2579.

Choi, H. J. & Lee, S. M. 2015 Heavy metal removal from acid mine drainage by calcined eggshell and microalgae hybrid system. *Environ. Sci. Pollut. Res.* **22**, 13404–13411.

Coles, C. A. & Yong, R. N. 2006 Use of equilibrium and initial metal concentrations in determining Freundlich isotherms for soils and sediments. *Eng. Geol.* **85**, 19–25.

Daraei, H., Mittal, A., Noorisepehr, M. & Mittal, J. 2013 Separation of chromium from water samples using eggshell powder as a low cost sorbent: kinetic and thermodynamic studies. *Desalin. Water Treat.* **53**, 1–7.

Ding, S. L., Li, Z. K. & Wang, R. 2010 Overview of dyeing wastewater treatment technology. *J. Water Resour. Protect.* **26**, 73–78.

Errais, E., Duplay, J., Darragi, F., M'Rabet, I., Aubert, A., Huber, F. & Morvan, G. 2011 Efficient anionic dye adsorption on natural untreated clay: kinetic study and thermodynamic parameters. *Desalination* **275**, 74–81.

Ghaly, A. E., Ananthashankar, R., Alhattab, M. & Ramakrishnan, V. V. 2014 Production, characterization and treatment of textile effluents: a critical review. *Chem. Eng. Process Technol.* **5** (1), 1–19.

Guru, P. S. & Dash, S. 2014 Sorption on eggshell waste – a review on ultrastructure, biomineralization and other applications. *Adv. Colloid Interface Sci.* **209**, 49–67.

Işmal, Ö. E., Yildirim, L. & Özdogan, E. 2014 Use of almond shell extracts plus biomordants as effective textile dye. *J. Clean. Prod.* **70**, 61–67.

Jin, L., Sun, Q., Xu, Q. & Xu, Y. 2015 Adsorptive removal of anionic dyes from aqueous solutions using microgel based on nanocellulose and polyvinylamine. *Bioresour. Technol.* **197**, 348–355.

Kim, D. Y., Oh, Y. K., Park, J. Y., Choi, S. A., Kim, B. H. & Han, J. I. 2015 An integrated process of microalgae harvesting and wet extraction using ferric coagulants. *Bioresour. Technol.* **191**, 469–474.

Lalhmunsiama, T. D. & Lee, S. M. 2016 Surface-functionalized activated sericite for the simultaneous removal of cadmium and phenol from aqueous solutions: mechanistic insights. *Chem. Eng. J.* **283**, 1414–1423.

Liu, L., Cheng, X. Z., Qin, P. & Pan, M. Y. 2012 Remove of Congo Red from wastewater by adsorption onto eggshell membrane. *Adv. Mater. Res.* **599**, 391–394.

Mahe, O., Briere, J. F. & Dez, I. 2015 Chitosan: an upgraded polysaccharide waste for organo catalysis. *Eur. J. Organic Chem.* **12**, 2559–2578.

Nguyen, T. A. & Juang, R. S. 2013 Treatment of waters and wastewaters containing sulfur dyes: a review. *Chem. Eng. J.* **219**, 109–117.

Ning, L. & Tao, L. 2011 Adsorption and decoloration of nitroso dye based on eggshell membrane. *Adv. Mater. Res.* **183–185**, 963–966.

Pettinato, M., Chakraborty, S., Arafat, H. A. & Calabro, V. 2015 Eggshell: a green adsorbent for heavy metal removal in an MBR system. *Ecotoxicol. Environ. Safety* **121**, 57–62.

Rohaizar, N. A., Hadi, N. A. & Sien, W. C. 2013 Removal of Cu(II) from water by adsorption on chicken eggshell. *Int. J. Eng. Technol.* **13**, 40–45.

Singha, B. & Das, S. K. 2011 Biosorption of Cr(VI) ions from aqueous solutions: kinetics, equilibrium, thermodynamics and desorption studies. *Colloids Surf. B* **84**, 221–232.

Tsai, W. T., Yang, J. M., Lai, C. W., Cheng, Y. H., Lin, C. C. & Yeh, C. M. 2006 Characterization and adsorption properties of eggshells and eggshell membrane. *Bioresour. Technol.* **97**, 488–493.

First received 17 October 2016; accepted in revised form 30 May 2017. Available online 26 July 2017